# Coproduction of Methanol and Dimethyl Ether from Biomass-Derived Syngas on a Cu–ZnO –Al 2 O 3 /γ-Al 2 O 3 Hybrid Catalyst

**ARTICLE** *in* ENERGY & FUELS · JANUARY 2008

Impact Factor: 2.79 · DOI: 10.1021/ef700461j



**4 AUTHORS**, INCLUDING:

Suk-Hwan Kang
Institute for advanced engineering, South K…

**60** PUBLICATIONS **666** CITATIONS

SEE PROFILE

# Coproduction of Methanol and Dimethyl Ether from Biomass-Derived Syngas on a Cu−ZnO−$Al_2O_3$/$\gamma$-$Al_2O_3$ Hybrid Catalyst

Jong-Wook Bae, H. S. Potdar, Suk-Hwan Kang, and Ki-Won Jun*

*Alternative Chemicals/Fuel Research Center, Korea Research Institute of Chemical Technology (KRICT), P.O. BOX 107, Yuseong, Daejeon, 305-600, Korea*

*Received August 1, 2007. Revised Manuscript Received October 7, 2007*

The coproduction of methanol (MeOH) and dimethyl ether (DME) from biomass-derived synthesis gas on the coprecipitated Cu−ZnO−$Al_2O_3$/$\gamma$-$Al_2O_3$ hybrid catalysts has been investigated to overcome the equilibrium conversion of CO on the MeOH only synthetic reaction at the $H_2$-decificient condition. Two different types of $\gamma$-$Al_2O_3$ were employed as the solid-acid component of hybrid catalyst: one prepared by a precipitation method and the other prepared by a sol–gel method. Several hybrid catalysts were prepared by the coprecipitation method in the slurry of $\gamma$-$Al_2O_3$ with the variation in the weight ratio of MeOH synthesis catalyst (Cu−ZnO−$Al_2O_3$) to solid-acid catalyst ($\gamma$-$Al_2O_3$) as well as by changing aging time during synthesis. The catalytic activity results revealed that the best yield of MeOH and DME with concomitant decrease in the $CO_2$ formation was obtained on the hybrid catalyst containing $\gamma$-$Al_2O_3$ prepared by the sol–gel method with an aging time of 6 h. The hybrid catalysts were characterized by using the BET surface area measurements, $NH_3$ temperature programmed desorption ($NH_3$-TPD), scanning electron microscopy (SEM), temperature programmed reduction (TPR), and X-ray diffraction (XRD) methods. The observed catalytic properties were related to the surface area of Cu metal, dispersion of Cu−ZnO−$Al_2O_3$ particles, and reducibility and acidity of hybrid catalysts. The enhanced catalytic activity with low selectivity to $CO_2$ is attributed to the facile reducibility of well-dispersed copper oxides at low temperatures and also to the benign acid strength of the hybrid catalysts.

## 1. Introduction

Synthesis gas (syngas), which is dominantly employed in the commercial scale synthesis of methanol (MeOH) and dimethyl ether (DME), could be produced from natural gas, coal, and (or) biomass gasification. In addition, biomass-derived $H_2$-deficient and $CO_2$-abundant syngas produced by gasification has been gaining more attention for MeOH and DME synthesis due to their application for renewable energy sources and high potential toward $CO_2$ reduction, which prevent global warming as well.[1] MeOH is an important raw material in chemical industries such as the starting feedstock for C1 chemistry and MeOH-to-gasoline (MTG)/MeOH-to-olefins (MTO) processes.[2,3] DME is also one of the attractive candidates for the production of dimethyl sulfate, methyl acetate, light olefins, and alternative clean fuels.[4–7] The commercialized two-step indirect process for the production of DME involves dehydration of MeOH on solid-acid catalysts like $\gamma$-$Al_2O_3$ or modified ZSM-5 zeolite,[8–10] which was previously synthesized by CO and/or $CO_2$ hydrogenation on Cu−ZnO-based catalysts.[11–16] Recently, many researchers have explored the development of a simple one-step direct process to produce DME from syngas on the hybrid catalysts mainly composed of (i) MeOH synthesis catalysts and (ii) solid-acid catalysts.[17–28]

* To whom correspondence should be addressed. E-mail: kwjun@krict.re.kr. Tel: 82-42-860-7671. (Fax) 82-42-860-7388.

(1) Hu, J.; Wang, Y.; Cao, C.; Elliott, D. C.; Stevens, D. J.; White, J. F. *Ind. Eng. Chem. Res.* **2005**, *44*, 1722–1727.
(2) Fujiwara, M.; Kieffer, R.; Ando, H.; Xu, Q.; Souma, Y. *Appl. Catal., A* **1997**, *154*, 87–101.
(3) Wu, X.; Abraha, M. G.; Anthony, R. G. *Appl. Catal., A* **2004**, *206*, 63–69.
(4) Semelsberger, T. A.; Borup, R. L.; Greene, H. L. *J. Power Sources* **2006**, *156*, 497–511.
(5) Cai, G.; Liu, Z.; Shi, R.; He, C.; Yang, L.; Sun, C.; Chang, Y. *Appl. Catal., A* **1995**, *125*, 29–38.
(6) Holladay, J. D.; Wang, Y.; Jones, E. *Chem. Rev.* **2004**, *104*, 4767–4790.
(7) Lee, S.; Sardesai, A. *Top. Catal.* **2005**, *32*, 197–207.
(8) Fu, Y.; Hong, T.; Chen, J.; Auroux, A.; Shen, J. *Thermochim. Acta* **2005**, *434*, 22–26.
(9) Kim, S. D.; Baek, S. C.; Lee, Y. H.; Jun, K. W.; Kim, M. J.; Yoo, I. S. *Appl. Catal., A* **2006**, *309*, 139–143.
(10) Blaszkowski, S. R.; van Santen, R. A. *J. Phys. Chem. B* **1997**, *101*, 2292–2305.
(11) Li, J. L.; Inui, T. *Appl. Catal., A* **1996**, *137*, 105–117.
(12) Ma, L.; Tran, T.; Wainwright, M. S. *Top. Catal.* **2003**, *22*, 295–304.
(13) Jun, K. W.; Shen, W. J.; Rama Rao, K. S.; Lee, K. W. *Appl. Catal., A* **1998**, *174*, 231–238.
(14) Nakamura, J.; Nakamura, I.; Uchijima, T. *Catal. Lett.* **1995**, *31*, 325–331.
(15) Yang, C.; Ma, Z.; Zhao, N.; Wei, W.; Hu, T.; Sun, Y. *Catal. Today* **2006**, *115*, 222–227.
(16) Sloczynski, J.; Grabowski, R.; Olszewski, P.; Kozlowska, A.; Stoch, J.; Lachowska, M.; Skrzypek, J. *Appl. Catal., A* **2006**, *310*, 127–137.
(17) Wang, L.; Fang, D.; Huang, X.; Zhang, S.; Qi, Y.; Liu, Z. *J. Nat. Gas Chem.* **2006**, *15*, 38–44.
(18) Moradi, G. R.; Nosrati, S.; Yaripor, F. *Catal. Commun.* **2007**, *8*, 598–606.
(19) Mao, D.; Yang, W.; Xia, J.; Zhang, B.; Lu, G. *J. Mol. Catal. A* **2006**, *250*, 138–144.
(20) Li, J. L.; Zhang, X. G.; Inui, T. *Appl. Catal., A* **1996**, *147*, 23–33.
(21) Ramos, F. S.; Duarte de Farias, A. M.; Borges, L. E. P; Monteiro, J. L.; Fraga, M. A.; Sousa-Aguiar, E. F.; Appel, L. G. *Catal. Today* **2005**, *101*, 39–44.
(22) Fei, J. H.; Yang, M. X.; Hou, Z. Y.; Zheng, X. M. *Energy Fuels* **2004**, *18*, 1584–1587.
(23) Wang, L.; Qi, Y.; Wei, Y.; Fang, D.; Meng, S.; Liu, Z. *Catal. Lett.* **2006**, *106*, 61–66.
(24) Xia, J.; Mao, D.; Zhang, B.; Chen, Q.; Tang, Y. *Catal. Lett.* **2004**, *98*, 235–240.
(25) Takeguchi, T.; Yanagisawa, K. I.; Inui, T.; Inoue, M. *Appl. Catal., A* **2000**, *192*, 201–209.

10.1021/ef700461j CCC: $40.75 
Published on Web 11/15/2007

It has been reported in the literature that the catalytic activity of hybrid catalysts could be properly explained by the dispersion of Cu particles, the crystallinity of MeOH synthesis catalysts, the acidic properties of solid-acid catalysts,[8,9,19,21,23–25,27] and the adsorption behavior of $H_2O$ and $CO_2$.[7,8,16,17,28] These properties of hybrid catalysts could be largely altered by the catalyst preparation methods such as the following: (i) precipitation at the optimum pH (∼7.0) and aging temperature (>70 °C),[11] (ii) preparation of highly dispersed fine crystallites and a high surface area of skeletal Cu by changing variables,[12,13,20,22] (iii) stabilization of active Cu species by adding promoters,[15,22,26] (iv) modification of surface acidity on the solid-acid catalyst by adding $Ti(SO_4)_2$ on $\gamma$-$Al_2O_3$,[8] Na on ZSM-5,[9] sulfate on $\gamma$-$Al_2O_3$,[19] Fe on ZSM-5,[24] and Mg on ZSM-5,[27] and (v) changes of silica–alumina ratio in zeolites.[25] The modification of surface acidity is an important control variable to enhance the DME selectivity. To prevent the hydrocarbon formation by dehydration of DME on the strong acidic sites, the hybrid catalysts should be properly designed to have benign acidic sites especially like Brønsted acidic sites. In addition, the control of surface acidity is an important variable since water could be strongly adsorbed on Lewis acidic sites and $CO_2$ could be formed by MeOH reforming or the water−gas shift (WGS) reaction on the strong acidic sites.[3,19,21] It was recently reported that the WGS reaction could be inhibited only at a high partial pressure of $CO_2$ and resulted in enhancing the selectivity toward desired products such as MeOH and DME.[7,17]

To design and develop proper hybrid catalysts for the direct DME synthesis from syngas, some researchers have focused their attention on the modification of solid-acid catalysts.[8,9,19,24,25,27] However, there is no investigation carried out so far using a simple method by varying the aging time during hybrid catalyst preparation to control the surface acidity and by optimization of particle size to enhance the selectivity to DME and MeOH with low $CO_2$ formation. The present study focuses on finding the proper preparation methods of hybrid catalyst Cu−ZnO−$Al_2O_3$/$\gamma$-$Al_2O_3$ during the synthesis to develop highly active and stable hybrid catalysts, which can work even in the biomass-derived syngas environments of $CO_2$-abundant and $H_2$-deficient conditions. Another aspect of the present work is to characterize hybrid catalysts by using various methods such as BET surface area measurement, temperature programmed desorption ($NH_3$-TPD), scanning electron microscopy (SEM), temperature programmed reduction (TPR), X-ray diffraction (XRD), and Cu surface area measurements and relate these findings with catalytic behaviors. All these results pertaining to synthesis, characterization, and performance of hybrid catalyst are presented in this paper.

## 2. Experimental Details

**2.1. Synthesis of Solid-Acid Catalysts.** Two types of $\gamma$-$Al_2O_3$ were synthesized by precipitation and the sol–gel method using two different aluminum precursors. In the first case, $\gamma$-$Al_2O_3$ powder was prepared from aluminum nitrate ($Al(NO_3)_3 \cdot 9H_2O$; AN; Aldrich) with a precipitant of sodium carbonate ($Na_2CO_3$; Junsei) by the conventional precipitation method.[29] The temperature was kept at ∼70 °C during precipitation as well as during the aging/digestion step. The pH of solution was maintained in the range of 7.5–8.5, and the precipitates were further digested at ∼70 °C for 3 h. The digested precipitates were filtered and washed with 2 L of hot deionized water. The dried precipitates were calcined at 550 °C for 5 h in air with a heating rate of 2 °C/min and resulted in the generation of $\gamma$-$Al_2O_3$ powder. In the second case, $\gamma$-$Al_2O_3$ powder was prepared from aluminum isopropoxide ($Al[OCH(CH_3)_2]_3$); AIP; Aldrich), acetic acid (AA), and 2-propanol as starting precursors by the sol–gel method.[30] In this method, initially, AIP was dissolved in 2-propanol with continuous stirring and the desired amount of AA and water were slowly added to the above stirred solution. The fast hydrolysis and slow condensation reactions occurred to precipitate Al in the form of fine hydroxide gel precipitate which was further aged/digested at ∼80 °C for 20 h. The molar ratio of AA/AIP was kept around 0.1, and the molar ratio of $H_2O$/AIP was kept around 3 during the preparation. The product thus obtained was washed several times with 2-propanol and finally dried at 80 °C in vacuum oven for 12 h. The as-dried precipitates were calcined in a flow of air at 500 °C for 5 h with a heating rate of 2 °C/min to obtain $\gamma$-$Al_2O_3$ powder. The $\gamma$-$Al_2O_3$ powder prepared using the above two methods with different aluminum precursors were employed to prepare the next hybrid catalysts.

**2.2. Preparation of Hybrid Catalysts.** The hybrid catalyst composed of Cu−ZnO−$Al_2O_3$/$\gamma$-$Al_2O_3$ was prepared by coprecipitation in the slurry of $\gamma$-$Al_2O_3$ powder. In the present study, the metal oxides composition consisting of 50 wt % CuO, 40 wt % ZnO, and 10 wt % $Al_2O_3$ for Cu−ZnO−$Al_2O_3$ was selected. The weight ratio of MeOH synthesis catalyst (Cu−ZnO−$Al_2O_3$) to solid-acid catalyst ($\gamma$-$Al_2O_3$) was varied from 1 to 5 to discover a correlation with the yield of desired products such as MeOH and DME and the weight ratio of them. For the synthesis of Cu−ZnO−$Al_2O_3$ catalyst, 5.03 g of copper acetate monohydrate, 4.31 g of zinc acetate dihydrate, and 2.94 g of aluminum nitrate were dissolved in 600 mL of deioinzed water. The pH of mixed metals solution was found to be in the range of 5.1–5.5. The solution of sodium carbonate was made separately by dissolving 8.34 g in 600 mL of deionized water to get the pH in the range of 10.5–11.0. The required quantity of previously synthesized $\gamma$-$Al_2O_3$ powder was added to a 200 mL of deionized water taken in a 2 L flask while stirring at ∼70 °C. Then, mixed metal precursor solution containing copper acetate, zinc acetate, and aluminum nitrate and sodium carbonate solution were added separately through a syringe pump with precise control of the feeding rate. The temperature was maintained at ∼70 °C during the precipitation, and the pH measured after precipitation was found to be in the range of 7.5–8.0. The slurry was further digested at ∼70 °C from 1 to 9 h. The precipitates were filtered, washed with hot deionized water, and extruded to the size of ∼2 mm before drying for 16 h at room temperature. The material was further dried in an oven at 110 °C for 12 h and subsequently calcined at 350 °C for 5 h in air.

**2.3. Catalyst Characterization.** The BET surface areas and pore volumes were estimated from nitrogen adsorption and desorption isotherm data obtained at –196 °C using a constant-volume adsorption apparatus (Micromeritics, ASAP-2400). The pore volumes were determined at a relative pressure ($P/P_o$) of 0.99. The calcined samples were degassed at 300 °C with a He flow for 4 h before measurements. The pore size distributions of samples were determined by a BJH (Barett−Joyner−Halenda) model from the desorption branch of the nitrogen isotherms.

The temperature programmed desorption of ammonia ($NH_3$-TPD) experiments were performed to determine the surface acidity of various hybrid catalysts. About 0.1 g of the samples was flushed initially with a He flow at 250 °C for 2 h, cooled to 100 °C, and saturated with $NH_3$. After $NH_3$ exposure, the sample was purged with a He flow until equilibrium, and then, TPD experiments were carried out from 100 to 600 °C at a heating rate of 10 °C/min.

The Cu surface area (defined as $S_{Cu}$ = exposed metallic copper area ($m^2$)/gram of sample) was measured by the $N_2O$ surface titration method. Prior to $N_2O$ titration, the samples were reduced

(26) Sun, K.; Lu, W.; Qiu, F.; Liu, S.; Xu, X. *Appl. Catal., A* **2003**, *252*, 243–249.
(27) Mao, D.; Yang, J.; Xia, W.; Zhang, B.; Song, Q.; Chen, Q. *J. Catal.* **2005**, *230*, 140–149.
(28) Aguayo, A. T.; Erena, J.; Sierra, I.; Olazar, M.; Bilbao, J. *Catal. Today* **2005**, *106*, 265–270.
(29) Potdar, H. S.; Jun, K. W.; Bae, J. W.; Kim, S. M.; Lee, Y. J. *Appl. Catal., A* **2007**, *321*, 109–116.
(30) Kim, S. M.; Lee, Y. J.; Jun, K. W.; Park, J. Y.; Potdar, H. S. *Mater. Chem. Phys.* **2005**, *104*, 56–61.

at 250 °C for 4 h with 5%$H_2/N_2$ flow, followed by purging and cooling with a He flow to 100 °C. The consumption of $N_2O$ and the evolution of $N_2$ on the metallic Cu sites ($N_2O + 2Cu = Cu_2O + N_2$) were analyzed by a thermal conductivity detector (TCD). The surface area of metallic Cu was calculated by assuming $1.46 \times 10^{19}$ Cu atoms/$m^2$ and a molar stoichiometry $N_2O/Cu_s$ (Cu atom on the surface) of 0.5.[31]

The powder X-ray diffraction (XRD) patterns were obtained with a Rigaku diffractometer using Cu Kα radiation to identify the phases of hybrid catalysts and their crystallinity. The morphology and surface compositions of hybrid catalysts were also characterized by using scanning electron microscopy (SEM; JEOL (JSM6700F)) and energy dispersive spectroscopy (EDS).

The temperature programmed reduction (TPR) experiments were performed to determine the reducibility of the surface metal oxides of hybrid catalysts. The samples were previously pretreated in a He flow up to 350 °C and kept for 2 h to remove the adsorbed water and other contaminants followed by cooling to 50 °C. The 5%$H_2$/He mixture was passed over the samples at a flow rate of 30 mL/min with the heating rate of 10 °C/min up to 500 °C. The effluent gas was passed over a molecular sieve trap to remove the generated water and analyzed by a GC equipped with a TCD.

**2.4. Catalytic Activity Tests.** The catalytic activity measurements were conducted in a fixed-bed stainless-steel reactor with a diameter of 12.7 mm using 1.0 g of pellet-form hybrid catalysts. Prior to catalytic experiments, all the catalysts were reduced by using a 5% $H_2/N_2$ flow at 250 °C for 4 h under atmospheric pressure. On the basis of other research for biomass gasification,[32] the mixed gas of $CO/CO_2/H_2$ (41/21/38 vol %) was selected as a model composition for biomass-derived syngas. The following reaction conditions were employed during the activity test: $T =$ 250 °C; $P = 40$ bar; space velocity (SV) = 11 000 1/h. The effluent products were analyzed by an online GC (DS6200, Donam Co.) equipped with Porapack-Q column connected to a TCD and simultaneously with a GS-Q column to a flame ionization detector (FID). The data shown in the present work are the averaged values taken from the results showing stable conversion of CO and selectivity to the products.

## 3. Results and Discussion

The commercialized process of DME production is composed of three important processes such as (i) syngas production by natural gas and (or) coal gasification and (ii) syngas to MeOH synthesis by CO and (or) $CO_2$ hydrogenation followed by (iii) dehydration of MeOH to DME on solid-acid catalysts. The main reactions involved in DME synthesis from syngas are represented by the following three reactions:

MeOH synthesis: $CO + 2H_2 \rightleftarrows CH_3OH$

$$\Delta H^\circ = -90.6 \text{ kJ/mol} \quad (1)$$

MeOH dehydration: $2CH_3OH \rightleftarrows CH_3OCH_3 + H_2O$

$$\Delta H^\circ = -23.4 \text{ kJ/mol} \quad (2)$$

WGS reaction: $H_2O + CO \rightleftarrows H_2 + CO_2$

$$\Delta H^\circ = -41.2 \text{ kJ/mol} \quad (3)$$

Total net reaction: $3CO + 3H_2 \rightleftarrows CH_3OCH_3 + CO_2$

$$\Delta H^\circ = -245.8 \text{ kJ/mol} \quad (4)$$

As predicted from the above thermodynamic data, the total net reaction (eq 4) is more thermodynamically favorable compared to the others (eqs 1, 2, and 3). The main advantages of the direct synthetic route to DME is surpassing the equilibrium constraint of the MeOH synthesis reaction by the in situ generation of extra hydrogen through the WGS reaction (eq 3) resulting in higher conversion of CO. The equilibrium conversion of CO on the MeOH only synthetic reaction is reported around 40% at the mole ratio of $H_2/CO = 2$, and CO conversion is much lower in the $H_2$-deficient condition.[20] In addition, DME synthesis from syngas could be controlled by the kinetics and (or) by thermodynamics. The equilibrium conversion of CO could be much higher in DME synthesis than in MeOH synthesis, and the products distribution could be altered with the extent of WGS activity.[20,33,34] In similar reaction conditions with our systems, the reported equilibrium conversion of CO is around 85%, more than 95% for MeOH dehydration to DME, and the probability of $CO_2$ hydrogenation to MeOH is trivial due to the $H_2$-deficient conditions and higher formation rate of $CO_2$ by the WGS reaction.[33,34] Since DME synthesis from syngas could be controlled by kinetics at a much higher space velocity and $CO_2$ concentration due to an inefficient removal of water by the WGS reaction,[33] the coproduction of MeOH and DME could be mainly controlled by kinetics rather than thermodynamics at $CO_2$-rich and $H_2$-deficient reaction conditions. To employ the hybrid catalysts for direct DME synthesis at the biomass-derived model composition of $CO/CO_2/H_2 = 41/21/38$, the catalysts should possess proper active sites for MeOH synthesis and also subsequent dehydration of MeOH to DME as well. Indeed, the coproduction of methanol and DME on hybrid catalysts gives an improved conversion at the expense of high $CO_2$ formation. In the limited catalyst packing, the use of hybrid catalysts leads to the loss of methanol synthesis rate and the increase in $CO_2$ production, which is diminishing the advantages of the hybrid catalytic system. Therefore, the present study focuses on the way to get much improved conversion of CO as well as a moderate $CO_2$ formation in the coproduction of MeOH and DME from the $H_2$-deficient and $CO_2$-abundant syngas employing the hybrid catalysts of Cu−ZnO−$Al_2O_3$/γ-$Al_2O_3$.

**3.1. Effects of Aluminum Precursors and Preparation Methods.** The results of the catalytic activity of Cu−ZnO−$Al_2O_3$ only and the physically mixed Cu−ZnO−$Al_2O_3$ (aging for 3 h) with γ-$Al_2O_3$ with the weight ratio of 2.3 were summarized in Table 1. On the Cu−ZnO−$Al_2O_3$ catalyst, CO conversion and MeOH selectivity are around 21.9% and 72.2%, separately. Furthermore, the physically mixed catalyst of Cu−ZnO−$Al_2O_3$ (aging for 3 h) with γ-$Al_2O_3$ from AIP at the weight ratio of 2.3 shows the high CO conversion around 34.1% and DME selectivity around 49.7%, but it shows a high selectivity to $CO_2$ around 40.1%. To find out proper reactivity (high conversion of CO and low selectivity to $CO_2$) in the hybrid catalysts, two different laboratory-made γ-$Al_2O_3$ were synthesized. The hybrid catalysts composed of Cu−ZnO−$Al_2O_3$/γ-$Al_2O_3$ were prepared by using two different types of γ-$Al_2O_3$ synthesized from two different aluminum precursors such as aluminum nitrate (AN) and aluminum isopropoxide (AIP). The details of the aluminum precursors employed and the aging time during the preparation of hybrid catalysts along with catalytic activities are summarized in Table 1. The hybrid catalyst of HDN-R3A3 was prepared by using the coprecipitation method with Cu, Zn, and Al precursors in the slurry of γ-$Al_2O_3$, which was previously synthesized from aluminum nitrate precursor for solid-acid catalyst, and HD-R3A3 was prepared from aluminum isopropoxide by the sol–gel method. In the notations of the above hybrid catalysts, HD denotes hybrid catalyst synthesized by using AIP (HDN by AN), R3 is for a weight

(31) Jensen, J. R.; Johannessen, T.; Livbjerg, H. *Appl. Catal., A* **2004**, *266*, 117–122.
(32) Ruggiero, M.; Manfrida, G. *Renewable Energy* **1999**, *16*, 1106–1109.
(33) Ng, K. L.; Chadwick, D.; Toseland, B. A. *Chem. Eng. Sci.* **1999**, *54*, 3587–3592.
(34) Jia, G.; Tan, Y.; Han, Y. *Ind. Eng. Chem. Res.* **2006**, *45*, 1152–1159.

**Table 1. Catalyst Notations and Catalytic Activities on the Differently Prepared Hybrid Catalysts[a]**

| notation | $Al_2O_3$ precursor[b] | cat. weight ratio | aging time (h) | CO conversion (mol %) | product distribution (mol %) | | | |
|---|---|---|---|---|---|---|---|---|
| | | | | | $CH_3OH$ | DME | $CO_2$ | byproducts[c] |
| $Cu-ZnO-Al_2O_3$ | | | 3 | 21.9 | 72.2 | 0.6 | 26.5 | 0.7 |
| HD-R3A3 (PM)[d] | AIP | 2.3 | 3 | 34.1 | 10.0 | 49.7 | 40.1 | 0.2 |
| HDN-R3A3 | AN | 2.3 | 3 | 23.0 | 43.1 | 22.1 | 34.3 | 0.5 |
| HD-R3A3 | AIP | 2.3 | 3 | 25.7 | 48.4 | 23.0 | 28.0 | 0.6 |
| HD-R1A3 | AIP | 1.0 | 3 | 17.8 | 25.5 | 44.0 | 30.2 | 0.3 |
| HD-R5A3 | AIP | 5.0 | 3 | 29.3 | 66.1 | 7.9 | 25.1 | 0.9 |
| HD-R3A1 | AIP | 2.3 | 1 | 20.0 | 35.4 | 24.2 | 39.7 | 0.7 |
| HD-R3A6 | AIP | 2.3 | 6 | 36.2 | 59.0 | 16.4 | 23.6 | 1.0 |
| HD-R3A9 | AIP | 2.3 | 9 | 30.6 | 44.3 | 24.3 | 30.8 | 0.6 |

[a] Reaction conditions: $T = 250$ °C; $P = 40$ bar; SV = 11 000 1/h; biomass-derived model feed composition of $CO/CO_2/H_2 = 41/21/38$. Catalyst notations of HD(N)-R#A# denote that HDN is a hybrid catalyst synthesized from aluminum nitrate precursor by coprecipitation, HD is a hybrid catalyst from aluminum isopropoxide by the sol−gel method, R# is the weight ratio of $Cu-ZnO-Al_2O_3$ to $\gamma$-$Al_2O_3$ catalyst, and A# is the aging time. [b] The abbreviation of AN stands for aluminum nitrate ($Al(NO_3)_3 \cdot 9H_2O$), and AIP is for aluminum isopropoxide ($Al[OCH(CH_3)_2]_3$). [c] Byproducts mainly include $CH_4$ and $C_2$ hydrocarbons. [d] The catalysts of $Cu-ZnO-Al_2O_3$ (aging for 3 h) and $\gamma$-$Al_2O_3$ from aluminum isopropoxide by the sol–gel method were physically mixed with the weight ratio of 2.3.

**Table 2. Results of $NH_3$-TPD for Synthesized $Al_2O_3$ from Two Different Precursors**

| notation | acidic sites | | | BET surface area ($m^2/g$) |
|---|---|---|---|---|
| | weak (mmol $NH_3$/g (%)) | strong (mmol $NH_3$/g (%)) | total (mmol $NH_3$/g) | |
| $Al_2O_3$ (AN) | 0.981 (58.7) | 0.689 (41.3) | 1.670 | 220.0 |
| $Al_2O_3$ (AIP) | 1.119 (63.3) | 0.648 (36.7) | 1.767 | 437.8 |

ratio of $Cu-ZnO-Al_2O_3$ to $\gamma$-$Al_2O_3$ of 3, and A3 is for a duration of aging time of 3 h. In general, the number of surface acidic sites as well as the acidic strength on solid-acid catalyst is responsible for MeOH dehydration activity. For example, the control of acidic strength of Brønsted acidic sites on $Al_2O_3$ surfaces by the modification with $Ti(SO_4)_2$ or sulfate could affect remarkably the rate of DME production and that of byproducts formation such as $CO_2$ and light hydrocarbons.[8,19,21,28] The two hybrid catalysts applied in the present study show a difference in selectivity toward $CO_2$ and MeOH formation; however, they are almost the same or marginally differ in the selectivity toward DME (Table 1). The results of $NH_3$-TPD (Table 2) suggest that the hybrid catalyst prepared from $\gamma$-$Al_2O_3$ using aluminum nitrate precursor shows strong acidic sites compared to the alumina prepared from AIP. These results are well explained by the previous reports that the formation of hydrocarbons and $CO_2$ could be more favorably induced on the more acidic sites by the water reforming of MeOH[19] and WGS. The CO conversion is not varied significantly for the hybrid catalysts prepared from two different aluminum precursors, although there is a large difference in BET surface area of $\gamma$-$Al_2O_3$ synthesized from AN (220.0 $m^2/g$) compared to $\gamma$-$Al_2O_3$ prepared from AIP (437.8 $m^2/g$). This could be due to the possible blockage of $\gamma$-$Al_2O_3$ micropores during the coprecipitation step of $Cu-ZnO-Al_2O_3$. Furthermore, the micropores of $\gamma$-$Al_2O_3$ with high surface area made from AIP could be much more easily blocked by $Cu-ZnO-Al_2O_3$ particles during the coprecipitation step. Therefore, the small differences in the final surface area of two differently synthesized hybrid catalysts are responsible for showing similar CO conversion with different product distributions due to the different characteristics of $\gamma$-$Al_2O_3$. On the basis of the above findings, we have selected $\gamma$-$Al_2O_3$ synthesized from AIP precursor showing a moderate amount of weak acidic sites as a solid-acid component and prepared the hybrid catalysts for further studies to discover the proper weight ratio of $Cu-ZnO-Al_2O_3$ to $\gamma$-$Al_2O_3$ catalyst and also the effects of aging times during the catalyst preparation on the catalytic performance.

**3.2. Effect of the Weight Ratio of $Cu-ZnO-Al_2O_3$ to $\gamma$-$Al_2O_3$.** The rate of DME formation is strongly affected by the concentration of solid-acid component in the hybrid catalysts, and it can be enhanced by increasing the concentration of solid-acid components in the hybrid catalysts or using more acidic solid-acid components.[17,18,25] If the formation rate of DME by MeOH dehydration is increased, CO could be converted above the equilibrium conversion of MeOH synthesis reaction due to the availability of hydrogen produced by the WGS reaction.[1,10,18,21,22,27] As shown in Table 1, the differences in activities of HD-R1A3, HD-R3A3, and HD-R5A3, having different concentrations of solid-acid catalyst, could be well explained by those phenomena. HD-R5A3 composed of 16.6 wt % $\gamma$-$Al_2O_3$ and 83.4 wt % $Cu-ZnO-Al_2O_3$ catalysts show higher selectivity toward MeOH (66.1%) with low DME (7.9%) and $CO_2$ (25.1%) selectivities. In contrast, HD-R1A3 composed of 50.0 wt % $\gamma$-$Al_2O_3$ and 50.0 wt % $Cu-ZnO-Al_2O_3$ catalysts show the lowest selectivity to MeOH (25.5%) along with highest DME (44.0%) and $CO_2$ (30.2%) selectivities. But, the conversion of CO increased by increasing the weight ratio of $Cu-ZnO-Al_2O_3$ to $\gamma$-$Al_2O_3$ catalyst due to the enhanced amount of $Cu-ZnO-Al_2O_3$ sites for MeOH synthesis reaction. Thus, MeOH synthesis could be the first step for DME synthesis from syngas in this series reaction. Furthermore, $CO_2$ formation is inversely related with weight ratio of $Cu-ZnO-Al_2O_3$ to $\gamma$-$Al_2O_3$ catalyst by reducing WGS activity on acidic sites. Interestingly, all the laboratory-made hybrid catalysts show a bimodal pore size distribution with pore diameters around 10−60 nm (Figure 1). With the increase of the weight ratio of $Cu-ZnO-Al_2O_3$ to $\gamma$-$Al_2O_3$ catalyst, the fraction of large pores around 60 nm increased and the opposite is true of small pores around 10 nm. From the above pore size distribution observations, we envisage that the large pores in hybrid catalyst are probably induced from the intragrain structures of $Cu-ZnO-Al_2O_3$ catalyst and the small pores arise from intergrain structures of $Cu-ZnO-Al_2O_3$ catalyst or $\gamma$-$Al_2O_3$ itself. The surface area of hybrid catalysts also decreased to 140.5 $m^2/g$ for HD-R1A3, 91.7 $m^2/g$ for HD-R3A3, and 87.1 $m^2/g$ for HD-R5A3 with increasing $Cu-ZnO-Al_2O_3$ concentration. As shown in Figure 2, CO conversion and MeOH selectivity is inversely correlating with the different pore volume ratio (small to large pore), and the selectivity to DME and $CO_2$ show an opposite trend. It may be concluded that MeOH dehydration activity is enhanced on the acidic sites which is mainly originated from the small pores in $\gamma$-$Al_2O_3$ catalyst. The results of Figure 2 further suggest that the selectivity to MeOH

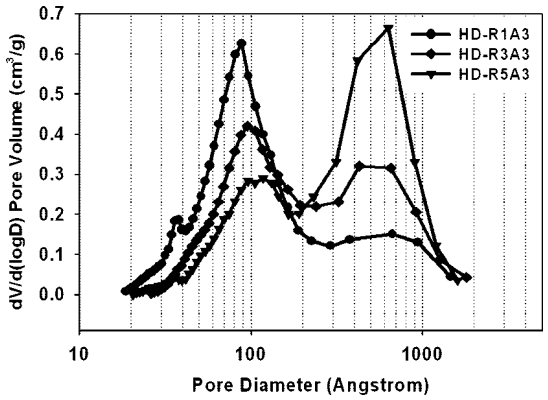


**Figure 1.** Pore size distribution (PSD) of hybrid catalysts with different weight ratios of Cu−ZnO−$Al_2O_3$ to $\gamma$-$Al_2O_3$ catalyst. The BET surface areas were as follows: 140.5 $m^2$/g for HD-R1A3, 91.7 $m^2$/g for HD-R3A3, and 87.1 $m^2$/g for HD-R5A3.

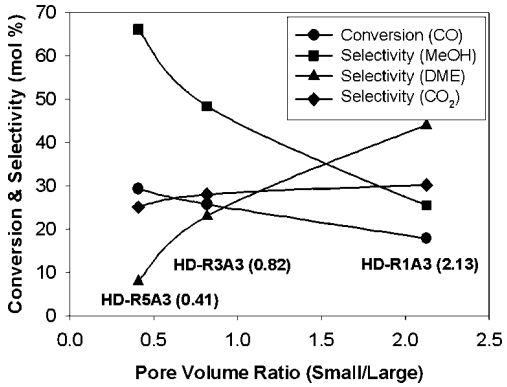


**Figure 2.** Conversion of CO and product distributions according to the pore volume ratio (small/large pore). The reaction conditions were as follows: $T$ = 250 °C; $P$ = 40 bar; SV = 11 000 1/h; biomass-derived model feed composition of $CO/CO_2/H_2$ = 41/21/38.

and DME is intersecting at the pore volume ratio of 1.5 and DME formation is found to be continuously increasing with the increase of small pores having a solid-acid character in spite of the gradually declining CO conversion. In a sort of consecutive reaction like direct DME synthesis from syngas, the partial pressure of previously formed MeOH could be the crucial factor for DME synthesis due to the lowest activation barrier for a concomitant two MeOH molecule adsorption pathway compared to that of a methoxy formation pathway from one MeOH adsorption.[10] Thus, results of the present study clearly suggest that DME formation is more favorable on the acidic sites adjusted by Cu−ZnO−$Al_2O_3$ particles in our hybrid catalysts and a large portion of small pores in the hybrid catalyst are intrinsically correlated with solid-acid sites on $\gamma$-$Al_2O_3$ surfaces.

**3.3. Effect of Aging Time on Hybrid Catalyst.** The particle size of Cu−ZnO−$Al_2O_3$ plays a decisive role on the catalytic activities as well as the surface acidity of hybrid catalysts.[8,13,16,18–20,26,35] To examine the effects of particle size and dispersion of Cu−ZnO−$Al_2O_3$ in hybrid catalysts, we have investigated the effects of the aging time during the preparation of hybrid catalysts. As described in the catalyst preparation section, the hybrid catalyst series of HD-R3A# was synthesized at a fixed weight ratio of Cu−ZnO−$Al_2O_3$ to $\gamma$-$Al_2O_3$ catalyst of 2.3, and at different aging times ranging from 1 to 9 h at the optimized pH and aging temperature.[11] In Cu/ZnO catalyst for the MeOH reforming reaction, it was reported that an average crystallite size of Cu/ZnO possessing homogeneous microstructure char-

(35) Kniep, B. L.; Girgsdies, F.; Ressler, T. *J. Catal.* **2005**, *236*, 34–44.

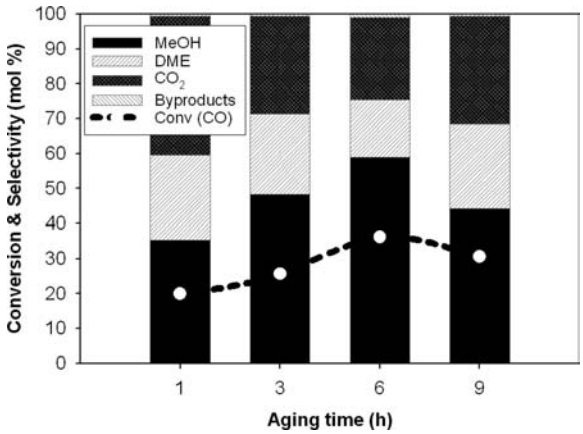


**Figure 3.** Conversion and products distribution on the hybrid catalysts with different aging times. The reaction conditions were as follows: $T$ = 250 °C; $P$ = 40 bar; SV = 11 000 1/h; biomass-derived model feed composition of $CO/CO_2/H_2$ = 41/21/38.

**Table 3. Textural Properties of Hybrid Catalysts Prepared at Different Aging Times**

| notation | surface area ($m^2$/g) | pore volume ($cm^3$/g) | avg. pore diameter (nm) |
|---|---|---|---|
| HD-R3A1 | 100.5 | 0.37 | 11.91 |
| HD-R3A3 | 91.7 | 0.42 | 15.07 |
| HD-R3A6 | 135.5 | 0.68 | 15.19 |
| HD-R3A9 | 110.1 | 0.56 | 16.69 |

acter decreased with the increase of aging time (above around 30 min) and resulted in the increase in catalytic activity.[35] In our hybrid catalysts as shown in Table 1 and Figure 3, CO conversion is maximized and the byproduct formation of $CO_2$ is minimized at 6 h of aging time. The catalyst performance was continuously enhanced up to the aging time of 6 h, and the selectivity to the desired products such as MeOH and DME was also concomitantly increased due to the reduced formation of $CO_2$. The CO conversion was enhanced from 20.0% for HD-R3A1 to the maximum value of 36.2% for HD-R3A6 and reduced again to 30.6% for HD-R3A9. In addition, the $CO_2$ and DME formation rate were also minimized on HD-R3A6 even in the conditions of higher CO conversion.

In order to understand the effect of aging time on the catalytic performance of our hybrid catalysts, the samples have been characterized by several characterization techniques such as BET surface area measurement, Cu surface area measurement by $N_2O$ pulse chemisorption, SEM and EDS analysis, XRD, $NH_3$-TPD, and TPR. In the HD-R3A# series, the BET surface area and pore volume were found to be higher for the 6 h aged HD-R3A6 catalyst showing 135.5 $m^2$/g and 0.68 $cm^3$/g (Table 3). The somewhat high surface area in HD-R3A1 ($S_g$ = 100.5 $m^2$/g) could be attributed to the well-developed micropore structure related to the smaller pore surface. The average pore diameter is continuously increasing with the increase of aging time possibly due to the good development of large pore structure in the hybrid catalysts and/or the sintering process of the deposited nanosized Cu−ZnO−$Al_2O_3$ particles on $\gamma$-$Al_2O_3$ surfaces. These findings are further confirmed by SEM analyses shown in Figure 4 for differently aged hybrid catalysts. The SEM results suggest that nanosized spheres are homogeneously dispersed on platelike materials in HD-R3A6 which is showing the highest CO conversion and MeOH selectivity. The sphere-type granules (I) are mainly composed of Cu−ZnO−$Al_2O_3$ catalyst and platelike materials (II) of solid-acid $\gamma$-$Al_2O_3$ catalyst which was also confirmed by EDS analysis (Figure 4). With increasing dispersion of sphere-type granules on plates-type

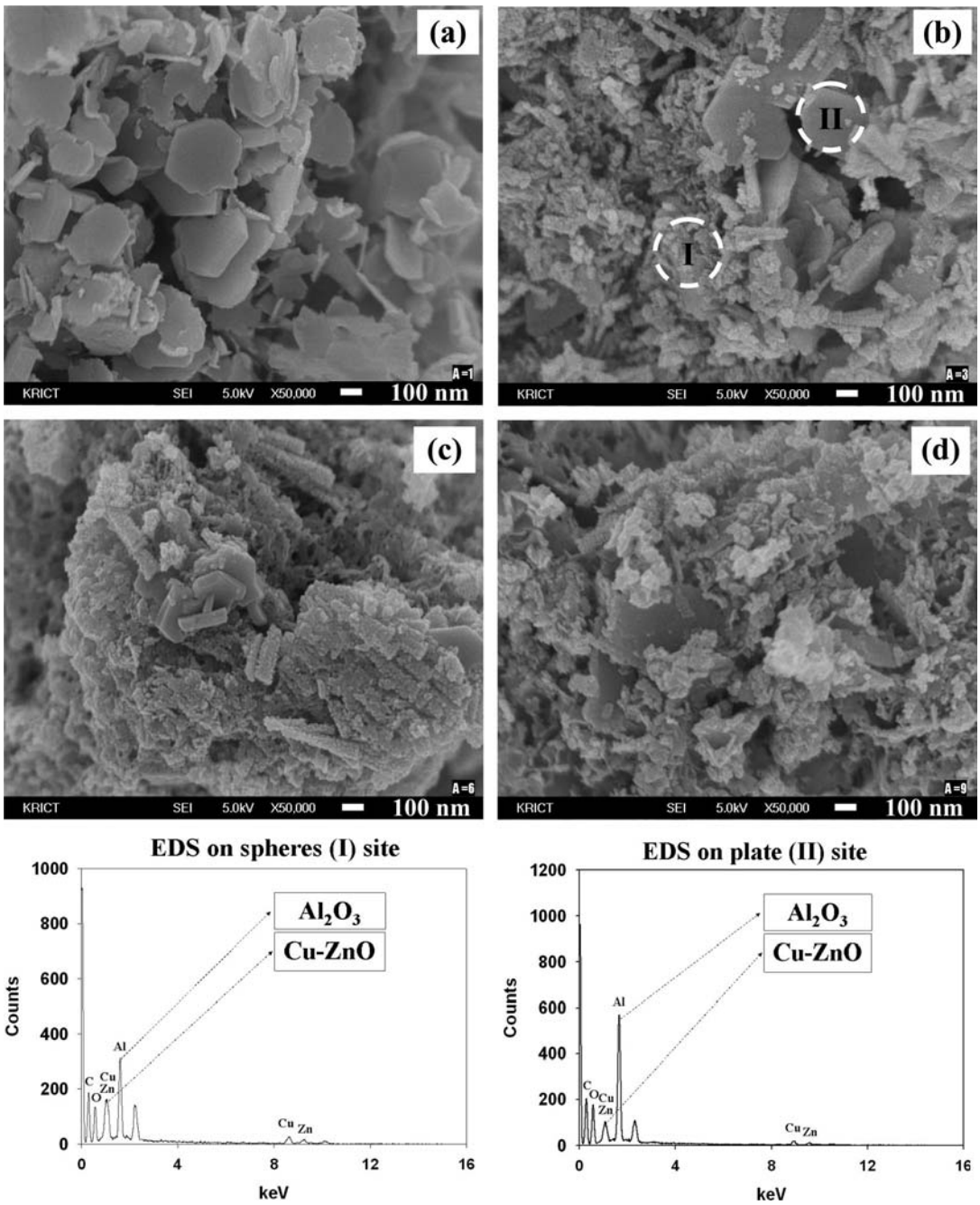


**Figure 4.** SEM analysis for surface morphologies of hybrid catalysts with different aging times and EDS analyses on HD-R3A3. (a) HD-R3A1. (b) HD-R3A3. (c) HD-R3A6. (d) HD-R3A9.

**Table 4. Results of $NH_3$-TPD of Hybrid Catalysts Prepared at Different Aging Times**

| | acid sites (mmol $NH_3$/g) | | |
|---|---|---|---|
| notation | weak (%) | strong (%) | total |
| HD-R3A1 | 1.049 (34.3) | 2.014 (65.7) | 3.063 |
| HD-R3A3 | 1.145 (53.3) | 1.004 (46.7) | 2.149 |
| HD-R3A6 | 1.273 (52.7) | 1.142 (47.3) | 2.415 |
| HD-R3A9 | 1.066 (47.1) | 1.202 (52.9) | 2.268 |

materials, the strong acidic sites which could be mainly originated from $\gamma$-$Al_2O_3$ surfaces were efficiently blocked as confirmed by $NH_3$-TPD results (Table 4 and Figure 5). The surface acidic sites and their strength could be directly correlated with the formation rate of $CO_2$ and DME.[8,9,22,23,25,36] For example, the $NH_3$-TPD results (Table 4) suggest that an increase of strong acidic sites (desorbed amount of $NH_3$ above 400 °C) from 1.142 mmol $NH_3$/g (HD-R3A6) to 2.014 mmol $NH_3$/g (HD-R3A1) resulted in the concomitant enhancement of $CO_2$ selectivity from 23.6% to 39.7%. Otherwise, the small changes in DME selectivity were found to be in the range of 23.0−24.3% for hybrid catalysts showing similar amounts of weak acidic sites in the range of 1.049−1.145 mmol $NH_3$/g. Although HD-R3A6 shows larger amounts of weak acidic sites, its selectivity to DME is minimized possibly owing to the lack of acidic strength of solid-acid sites for MeOH dehydration. Since maximum desorption temperatures of $NH_3$ ($T_{max}$) as well as the amounts of strong acidic sites have some direct correlation with $CO_2$ formation, HD-R3A6 shows the lowest desorption temperatures of $NH_3$ at 512 °C. This could be the possible reason for the formation of the least $CO_2$, and the opposite is true in HD-R3A1. Apparently, the presence of weak acidic sites could be correlated with MeOH dehydration and WGS reaction to

(36) Fu, Y.; Shen, J. *J. Catal.* **2007**, *248*, 101–110.

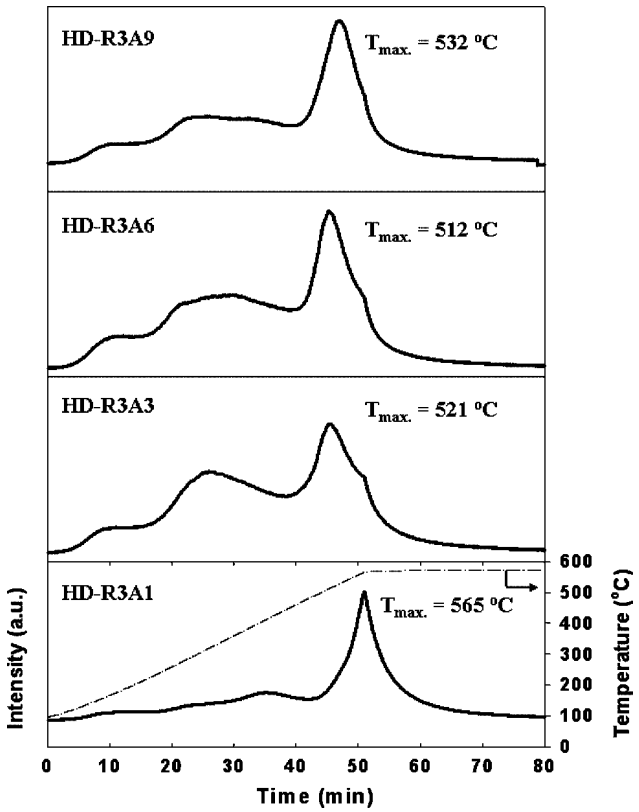


**Figure 5.** $NH_3$-TPD analyses on the differently aged hybrid catalysts.

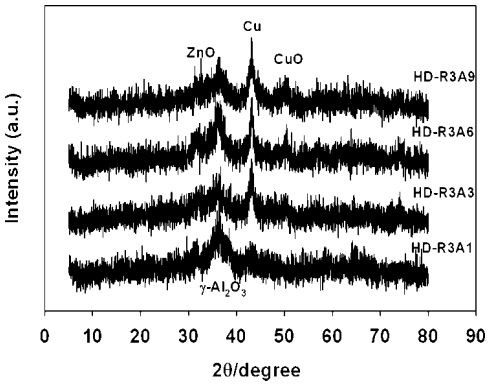


**Figure 6.** XRD patterns on the used hybrid catalysts with different aging times.

$CO_2$ formation in the presence of strong acidic sites. Since the catalytic acidic sites for DME and $CO_2$ formation could be easily blocked during Cu−ZnO−$Al_2O_3$ catalyst precipitation, the lower DME selectivity could be adequately explained on HD-R3A6, which shows highly dispersed sphere-type Cu−ZnO−$Al_2O_3$ particles. The HD-R3A9 prepared by a longer aging time for 9 h shows that sphere-type granule particles were sintered and agglomerated to ~50 nm in size. In contrast, sphere-type granule particles were not much observed in HD-R3A1 due to the possible strong interactions of Cu−ZnO−$Al_2O_3$ with $\gamma$-$Al_2O_3$ or the fact that oxidized Cu−ZnO−$Al_2O_3$ particles could not be formed completely at the calcination temperature around 350 °C. As shown in Figure 6, XRD analyses were conducted for the used hybrid catalysts (after reaction for more than 20 h). The Cu metal diffraction peak at $2\theta = 43.3°$ was observed in all the catalysts with the coexistence of CuO except for HD-R3A1. Although the dispersion of Cu−ZnO particles is an important factor for determining catalytic activity,[16,20,35] the reducibility is also a key parameter to assess catalyst perfor-

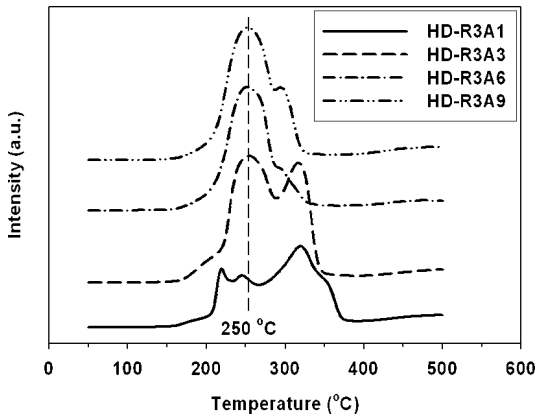


**Figure 7.** Temperature programmed reduction (TPR) profiles on the differently aged hybrid catalysts.

**Table 5. Cu Surface Area Measurements by Pulse Chemisorption of $N_2O$ and Calculated TOF Values**

| | | TOF (CO molecules to products/ ($Cu_{surf.atom}$ s)) × $10^{-1}$ | |
|---|---|---|---|
| notation | Cu surface area ($m^2$/g) | to MeOH + DME + $CO_2$ | to MeOH + DME |
| HD-R3A1 | 2.291 | 20.97 | 3.594 |
| HD-R3A3 | 3.388 | 15.91 | 3.539 |
| HD-R3A6 | 5.340 | 16.30 | 3.150 |
| HD-R3A9 | 4.572 | 16.13 | 3.465 |

mance. Furthermore, the smaller the well-developed nanosized Cu−ZnO−$Al_2O_3$ particles, the higher their reducibility as shown in Figure 7. HD-R3A1 shows three different $H_2$ consumption peaks during TPR at 220, 250, and 320 °C. The high-temperature reduction peak in this catalyst is much larger than the other catalysts. Thus, the low reducibility could be the main reason for exhibiting lower catalytic activity, and it could be induced from the nature of strong interactions of well-dispersed oxidized Cu−ZnO−$Al_2O_3$ particles on $\gamma$-$Al_2O_3$. As the dispersion of sphere-type granule particles increases, the intensity of the high-temperature reduction peak around 320 °C is reduced and the activity for MeOH synthesis is enhanced. In addition, the sintered Cu−ZnO−$Al_2O_3$ particles on HD-R3A9 show a shoulder peak at the somewhat high temperature of 300 °C and the catalyst activity is reduced concomitantly. The highly dispersed Cu−ZnO−$Al_2O_3$ particles possessing lower reduction probability like HD-R3A1 (confirmed by XRD and TPR) are responsible for exhibiting lower catalytic activity and higher $CO_2$ formation due to their strong acidic property. Therefore, in our hybrid catalysts, the small particle size of the Cu−ZnO−$Al_2O_3$ component as well as the reducibility at low temperature might have favored the enhancement of the activity of hybrid catalysts.

To calculate the turn-over frequency (TOF) of hybrid catalysts which were not showing equilibrium conversion of CO, the Cu surface area was measured by the pulse chemisorption method using $N_2O$ gas as a probe molecule, and the results are shown in Table 5. The Cu surface areas correlate well with the BET surface area and particle size of Cu−ZnO−$Al_2O_3$ catalyst, and the maximum Cu surface area is found to be around 5.340 $m^2$/g for HD-R3A6. The Cu surface area is an important factor for MeOH synthesis and further MeOH dehydration activity in this consecutive reaction. TOF values based on the total number of converted CO molecules are in the range of 1.591−2.097 CO molecules/($Cu_{surf.atom}$ s), and this value is minimized on HD-R3A1. Since a large portion of CO can be transformed to $CO_2$ by WGS reaction on acidic sites, HD-R3A1 possessing highly

dispersed Cu−ZnO−$Al_2O_3$ catalyst shows a higher TOF value. However, based on the CO converted to desired products such as MeOH and DME, the TOF values are found to be in the rage of 0.3150−0.3594 CO molecules/($Cu_{surf.atom}$ s) in all the hybrid catalysts. Similar TOF values are obtained irrespective of aging times which suggests that the concentration of well-dispersed Cu−ZnO−$Al_2O_3$ particles on $\gamma$-$Al_2O_3$ could be directly related to CO conversion and product distribution.

On the basis of the above findings, we have shown the facile control method of surface acidity on hybrid catalysts by simply changing the aging time during catalyst preparation. On the hybrid catalyst for direct DME synthesis from syngas, higher catalyst performance with low $CO_2$ formation could be obtained by developing highly dispersed Cu−ZnO−$Al_2O_3$ particles on solid-acid $\gamma$-$Al_2O_3$ surfaces possessing facile reducibility at low temperature and also benign acidic strength.

## 4. Conclusions

The following conclusions can be drawn from the present investigations dealing with the coprecipitated hybrid catalysts, Cu−ZnO−$Al_2O_3$/$\gamma$-$Al_2O_3$. Hybrid catalysts show bimodal pore size distribution, and each of the two different pore sizes seem to be related with a reaction—MeOH synthesis mainly occurs on large pores induced from the intragrain structures of Cu−ZnO−$Al_2O_3$ catalyst, while MeOH dehydration occurs on small pores induced from intergrain structures of Cu−ZnO−$Al_2O_3$ catalyst or $\gamma$-$Al_2O_3$ itself. The catalytic performance is largely dependent on the aging time during the preparation of the hybrid catalysts. The enhancement in the catalytic activity of the methanol synthesis function in the bifunctional catalyst causes a decrease of the DME production rate as well as $CO_2$ formation, and it can be achieved by optimizing the aging time, which is found to be 6 h in our hybrid catalyst. Although the coprecipitated Cu−ZnO−$Al_2O_3$ particles blocked the acid sites of $\gamma$-$Al_2O_3$, the hybrid catalysts of the deposited Cu−ZnO−$Al_2O_3$ on $\gamma$-$Al_2O_3$ give the improved methanol synthetic activity owing to the better dispersion of Cu−ZnO−$Al_2O_3$ particles. The enhanced activity is related to the Cu surface area, dispersion of Cu−ZnO−$Al_2O_3$ particles on $\gamma$-$Al_2O_3$ surfaces, reducibility of copper oxides, and surface acidity of hybrid catalysts. To achieve a catalyst showing the high activity to the desired products with low $CO_2$ formation, the hybrid catalysts should be designed to have well-dispersed sphere-type Cu−ZnO−$Al_2O_3$ particles on the solid-acid $\gamma$-$Al_2O_3$ surfaces having the characteristics of facile reducibility at low temperature and optimum surface acidity.

**Acknowledgment.** H.S.P. is thankful to KOFST for a Brain-Pool fellowship and to the Director of the National Chemical Laboratory, Pune-411008, for granting EOL for one year. We also thank Dr. K.V.R. Chary, visiting scientist under the KOFST Brain-Pool fellowship, for helpful discussions.

EF700461J